

UNIOSUN Journal of Engineering and Environmental Sciences. Vol. 6 No. 1. March. 2024

OPTIMAL LOCATION AND SIZING OF DG IN DISTRIBUTION NETWORK: IMPACT ON OVERCURRENT DISTRIBUTION PROTECTION SCHEME

Adeleye, A.O., Ajewole, T.O., Momoh, O.D.

Abstract The integration of distributed generation (DG) into the existing distribution networks minimizes active power losses and improves the voltage profile. The recent improvement in the development of DG technology has caused increase in the penetration of DG from different sources. The optimal location and sizing of DG is very challenging and introduces different protection issues. This is caused by penetration of current flow from different source which is contrary to the principles of operation of the conventional overcurrent scheme. This paper presents optimal method of DG placement and sizing using firefly algorithm and its impact of DG penetration on overcurrent protection scheme. Low voltage distribution network is modelled and simulated in PSCAD/EMTDC and DigSilent power factory software using IEEE 33 and Ayepe 34 standard bus. False tripping of feeders, Nuisance tripping, blinding of the protection scheme and unintentional islanding caused as result of Photovoltaic penetration into the distribution network were simulated. Coordination of overcurrent relays with and without DG penetration were analyzed and possible mitigation algorithm were proposed. The simulation result obtained showed that the proposed methods significantly improve the protection scheme coordination.

Keywords: Overcurrent relay, photovoltaic, protection coordination, distributed generation, firefly algorithm

I. Introduction

The penetration of DG into the distribution network provides several advantages such as power loss reduction due to the location of DGs at the load centers, global warming reduction due to green energy generation, improvement of voltage profile, improving power quality, higher energy operating efficiently and enhancement of network capacity [1]. However, the penetration of DG despite its advantages provides several issues to the overcurrent protection scheme normally

Adeleye, A. O., Ajewole, T. O,

(Department of Electrical and Electronic Engineering, Osun State University Osogbo, Nigeria.)

Momoh, O. D.

((School of Polytechnic, Purdue University Fort Wayne, U.S.A)

Corresponding Author: titus.ajewole@uniosun.edu.ng

adopted for the protection of the distribution network. The present conventional overcurrent protection scheme adopted is only modeled to operate for a radial distribution network with only directional power flow. To fully reap the benefits of DG integration, the appropriate allocation of the DG to be integrated into distribution networks are required [2]. The integration of DG optimally reduces system losses by up to 47%, power purchase costs by up to 92%, and energy not supplied costs by 40% [3]. Inappropriate DG allocation may diminish or increase system losses, cause unacceptable voltage variation, interfere with voltage control processes, and increase network capital and operating costs [4]. The optimal allocation of DG plays a very important role in

power loss reduction and network voltage The stability. DG optimal allocation essentially complex combinational a optimization problem that necessitates the simultaneous optimization of multiple objective functions. Several methods have been proposed by many researchers to allocate DG in the literature [5]. Ref. [6] allocated DG to abase power loss using the exact loss formula. The approach was applied to place a single DG when only the active power was supplied by the DG. Loss sensitivity factor-based methods were used to narrow the search field by choosing the potential places for a single DG deployment. However, multiple placements of DGs were not considered, and also, the DG was not optimally placed for loss reduction. An analytical technique was put out by [7], for figuring out the best sizes and placements for four distinct DG kinds. It was demonstrated that, to cut down on losses, the operational power factor of DGs was closer to the system's entire load's power factor. To best find DGs in a mesh network, [8] suggested a method based on the Hereford Ranch Algorithm. The suggested technique was utilized to assign DGs in the best possible way to maximize benefits while lowering active power losses in the system. The proposed approach was determined to be successful when the findings were contrasted with those from the traditional second approach and the genetic algorithm (GA). Ref. [9] has suggested a GA-based ideal DG size and location in distribution systems. Depending on bus admittance, generation data, and network load distribution, the GA approach was utilized to calculate the ideal size and position of DG in networks. In systems with 16, 37, and 75 buses, simulation results were used to evaluate the efficacy of the suggested approach. Undervoltage and line loading limits were used to

achieve the lowest possible transmission losses while loading the network uniformly. To determine the ideal position and capacity of DG units, [10] suggested using a differential evolution optimization technique. The major goals of integrating DG into the system are loss reduction and network voltage profile improvement. A single DG was subjected to the optimization procedure to determine its size and the position to reduce loss. Several DG allocations were not considered, though. For DG allocation, [11] employed an artificial neural network (ANN). To assess the stability of nodes, a voltage stability index (VSI) was created from a standard power flow equation. Finally, in order to find DG units, a priority list was created using VSI. The correct size of the DG units was then determined using the ANN approach to guarantee the allowed static voltage for each bus. The network's static voltage profile improved as a consequence; however, DG unit economic and geographic variables were not taken into account. For the optimal allocation of DG, the combination of GA and particle swarm optimization (PSO) has been suggested [12]. The MATLAB/PSAT toolbox was used for modeling and simulations of power systems, and the results revealed an improved steady state. Based the information collected through the literature search on the optimal location of DGs and their sizes, the analytical techniques are quick and simple to implement, but the results are only indicative, as well as facing the problem of an approximate solution. This problem has been investigated by many researchers, and were achieved with the improvements introduction of different heuristic optimization techniques that have not yet been described. Hence, this research developed a hybrid model conventional and that integrates nonconventional methods to optimize the location and size of DGs. However, the penetration of DGs to the distribution network transform the conventional radial distribution power flow into a meshed structure with bidirectional power flow which increases or decreases the network short circuit current values of different buses [13]. DG penetration affects or violates existing planning and operation practices. The insertion of DGs on different feeders resulted to the redistribution of fault current between the feeder supply and DGs. Hence, the load and fault current through the overcurrent protection relays may decrease, increase or remain the same. The size of fault current depends on the location of DG from the fault point. This condition will lead to the overcurrent protection scheme coordination breakdown and mal operation of the relays. In [14], the protection coordination is designed in a way to isolate only the faulty part of the distribution system upon occurrence of fault. This is called coordination of protection scheme. The penetration of DG in the distribution network if not properly coordinated causes the mal operation of coordination. Coordination of relay requires proper adjustment and coordination of time setting multipliers and pickup current setting. Research by [15] shows that in the past standard characteristics are manipulated rather than the pickup current and the time multiplier settings. Penetration of DG contributes to increase in the short circuit current level. Penetration of single DG may not really affect the level of short circuit current. however, penetration of multiple DGs increase the level of short circuit current which affect the conventional overcurrent protection scheme [16]. However, the influence of DG on overcurrent protection scheme depends on the level DG penetration into the distribution network. The major impact

of DG penetration on overcurrent protection scheme includes the following; reduction in the reach of the relays, miscoordination between different relays due to increase in the short circuit current which is the basis of calibration, unsynchronized reclosure, blinding of protection scheme, unintentional islanding and nuisance tripping [17]. Fuses are high speed overcurrent distribution network protection devices that need to be replaced each time the fuse melts. High level of DG penetration affects this device and caused regular replacement. DG penetration, if not well coordinated, affects the automatic recloser system which is used to clear transient faults in a distribution system. The protection system recloses the faulty section from the source end while the remote end is unenergized. However, with the presences of DG the system configuration will change to a loop or ring distribution system as the DG source will serves as another source which will cause the system to be energized from different source thereby obstructing the automatic recloser system. The operation of DG penetration is contrary to the principle of automatic recloser system [18]. Hence, this research developed a hybrid model that integrates conventional and non-conventional methods to optimize the location and size of DGs and equally study the impact of DG penetration on distribution overcurrent protection scheme.

II. Materials and Methods

This section of the article presents the conventional and non-conventional hybrid optimal location and size of DG in distribution networks. The conventional method uses the method of power loss stability index (PLSI), which uses the standard exact power loss equations while the hybrid model is a

combination of conventional and nonconventional methods. The conventional approach was utilized to establish the ideal sizes of DG units connected to various buses, while the nonconventional method was utilized to find the appropriate locations of the DGs that best improved the efficiency of networks. Prior to using the nonconventional method, the voltage stability index (VSI) was used to minimize the search space for optimal location of DG from which the firefly algorithm (FA) was adjusted to suit optimal DG placement in order to speed up the process of finding the distribution network's ideal DG site by performing a random search.

A. Voltage stability index

The VSI was utilized to obtain the bus that is most vulnerable to voltage collapse. The algorithm was used to determine the bus that requires urgent attention in order to avert system voltage collapse. The different branch currents and the power at each node were computed using Equations (1) and (2).

$$I(jj) = \frac{V(m1) - V(m2)}{r(ij) + ix(ij)} \tag{1}$$

Where, jj = branch number, m1 = branch end node, m2 = receiving end node, V(m1) = voltage of node 1, V(m2) = voltage of node m2.

$$P(m2) - jQ(m2) = V^*(m2)I(jj)$$
 (2)

P(m2) = total real power load fed through node m2, Q(m2) = total reactive power load fed through node m2, V(m2) = voltage of node m2.

Solving Equations (1) and (2), gives Equation (3).

$$||V(m2)|^{4} - \{|V(m1)|^{2} - 2P(m2)r(jj) - 2Q(m2)x(jj)\}|V(m2)|^{2} + \{P^{2}(m2) + Q^{2}(m2)\}\{r^{2}(jj) + x^{2}(jj)\} = 0$$
(3)

Setting

$$b(jj) = |V(m1)|^2 - 2P(m2)r(jj) - 2Q(m2)x(jj)\}$$
(1)

$$c(jj) = \{P^{2}(m2) + Q^{2}(m2)\}\{r^{2}(jj) + x^{2}(jj)\}$$
(2)

Putting Equations (4) and (5) into Equation (3) and rearranging gives Equation (6),

$$|V(m2)|^4 - b(jj)|V(m2)|^2 + c(jj)$$
= 0 (3)

From Equation (6), it can be observed that the receiving end voltage has four different solutions, which are presented in Equations (7) to (10).

$$0.707 [b(jj) + \{b^{2}(jj) - 4c(jj)\}^{1/2}]^{1/2}$$
 (7)

$$-0.707 [b(jj) - \{b^{2}(jj) - 4c(jj)\}^{1/2}]^{1/2}$$
(8)

$$-0.707 [b(jj) + \{b^{2}(jj) - 4c(jj)\}^{1/2}]^{1/2}$$
(9)

$$0.707 [b(jj) - \{b^{2}(jj) - 4c(jj)\}^{1/2}]^{1/2}$$
 (10)

Substituting the Equation (7) into Equation (6) gives Equation (11)

$$|V(m2)| = 0.707 \left[b(jj) + \{b^2(jj) - 4.0c(jj)\}^{\frac{1}{2}} \right]^{\frac{1}{2}}$$
(11)

The active and reactive power loss can be computed utilizing Equation (12) and (13).

$$LP(jj) = \frac{r(jj)\{P^2(m2) + Q^2(m2)\}}{|V(m2)|^2}$$
(12)

$$LQ(jj) = \frac{x(jj)\{P^2(m2) + Q^2(m2)\}}{|V(m2)|^2}$$
(13)

From Equation (11), load flow exists if

$$b^{2}(jj) - 4.0c(jj) \ge 0 \tag{14}$$

From Equations (4), (5) and (10), Equation (15) was obtained.

$$\{|V(m1)|^{2} - 2P(m2)r(jj) - 2Q(m2)x(jj)\}^{2} - 4.0\{P^{2}(m2) + Q^{2}(m2)\}\{r^{2}(jj) + x^{2}(jj)\} \ge 0$$
(15)

Simplifying Equation (15), Equation (16) was obtained.

$$V(m1)|^4 - 4.0\{P(m2)x(jj) - Q(m2)r(jj)\}^2 - 4.0\{P(m2)r(jj) + Q(m2)x(jj)\}|V(m1)|^2 \ge 0$$
 (16)
Equation (16) gives the voltage stability index.

B. Power loss minimization and optimum size of DG

The exact power loss minimization for each of the lines was determined using Equation (17).

$$P_{loss} = \sum_{i=1}^{N} \sum_{j=1}^{N} \left[\alpha_{ij} (P_i P_j + Q_i Q_j) - \beta_{ij} (Q_i P_j - P_i Q_j) \right]$$

$$(17)$$

Where, α_{ij} and β_{ij} are expressed in Equations (18) and (19).

$$\alpha_{ij} = \frac{r_{ij}}{V_i V_j} \cos(\delta_i - \delta_j)$$
 (18)

$$\beta_{ij} = \frac{r_{ij}}{V_i V_j} \sin(\delta_i - \delta_j) \tag{19}$$

Where, V_j and δ_j are the complex voltage magnitude and the angle at the bus i, r_{ij} +

 $jx_{ij} = Z_{ij}$ the ij^{th} element of Z bus impedance matrix, P_i and P_j are the active power injections at the i^{th} and j^{th} buses, Q_i and Q_j are the reactive power injections at the i^{th} and j^{th} buses. The optimum size of DG at each bus i for minimizing loss was calculated using Equation (21).

$$P_{DG_i}$$

$$= \frac{\alpha_{ii}(P_{D_i} + aQ_{D_i}) + \beta_{ii}(aP_{D_i} - Q_{D_i}) - X_i}{a^2\alpha_{ii} + \alpha_{ii}}$$
(21)

The power factor of DG depends on the operating conditions and the type of DG. For type 1 DG, the power factor is unity. i.e., $PF_{DG} = 0$ and a = 0. Therefore, Equation (21) is reduced to Equation (22).

$$P_{\mathrm{DG}_{i}} = P_{D_{i}} - \frac{1}{\alpha_{ii}} \left[\beta_{ii} Q_{D_{i}} + \sum_{\substack{j=1\\j\neq i}}^{N} (\alpha_{ij} P_{j} - \alpha_{ij} Q_{j}) \right]$$

$$(22)$$

For type 2 $PF_{DG} = 0$ and $\alpha = \infty$, hence, Equation (21) is reduced to Equation (23)

$$Q_{\mathrm{DG}_{i}} = Q_{D_{i}} + \frac{1}{\alpha_{ii}} \left[\beta_{ii} P_{D_{i}} + \sum_{\substack{j=1\\j\neq i}}^{N} (\alpha_{ij} Q_{j} - \beta_{ij} P_{j}) \right]$$

$$(234)$$

C. Hybrid algorithm

The hybrid model is a combination of conventional and nonconventional methods. The conventional approach was utilized to establish the ideal sizes of DG units connected to various buses as presented in Equations (22) and (23), while the nonconventional method was utilized to determine the appropriate location of the DGs that best improved the efficiency of the network as presented in the hybrid algorithm of Figure 1. Prior to using the nonconventional method, the VSI as presented in the equations were used to minimize the search space for optimal location of DG from which the FA was used to adjust the optimal DG placement in order to speed up the process of finding the distribution network's ideal DG site by performing a random search.

i. Firefly Algorithm

The FA is a nature-inspired meta-heuristic optimization technique that utilizes social (flashing) firefly behavior. This flashing light may be linked to the objective function that must be maximized, allowing for the development of novel optimization techniques. Although firefly shares many characteristics

with previous approaches depending on "swarm intelligence," it is far easier in both idea and execution. For a maximizing problem, the brightness can easily be related to the value of the objective function. Other types of brightness can be specified in the same way that the fitness function in GA or the bacterial foraging algorithm can. The fluctuations in light

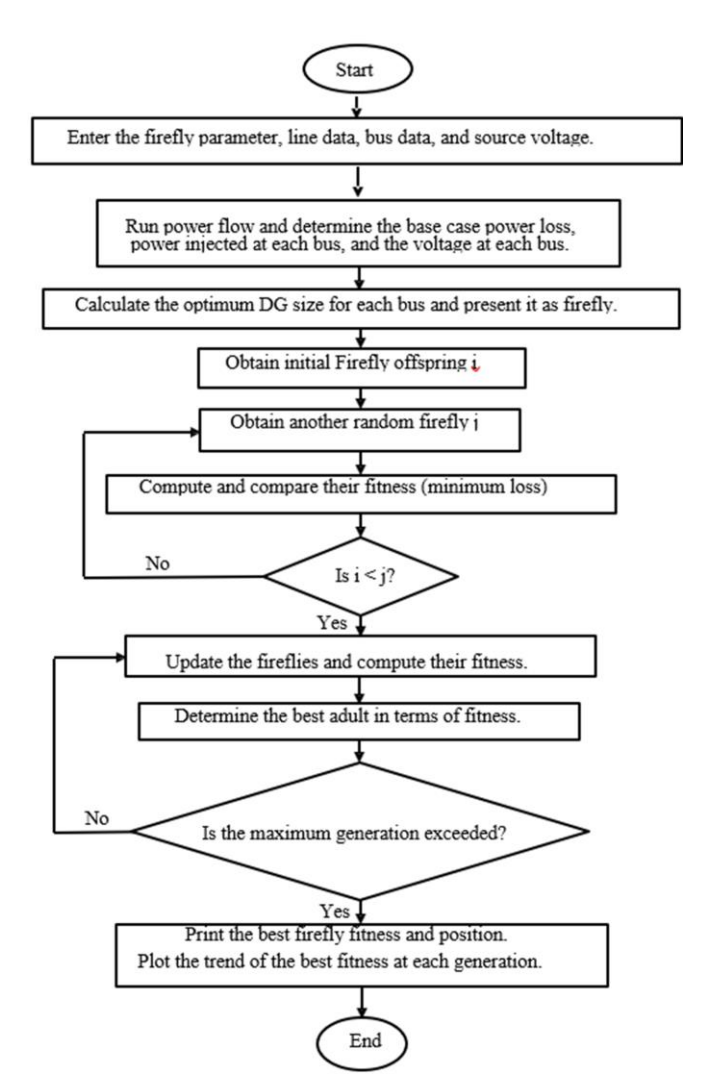


Figure 1: Flowchart of the Hybrid Algorithm

intensity and attractiveness follow monotonically decreasing functions since they diminish as the distance from the source widens. The gaussian function I(r), r the distance between any two fireflies, I_0 , which is the original light intensity, γ and β_0 , which are the attractiveness values were all assumed.

The objective function was formulated as presented in Equation (24) by minimizing the total power loss in a distribution network as defined in Equation (17).

$$(x) = \min(\sum_{i=1}^{n} P_{loss}) \tag{17}$$

f(x) is the optimal result obtained after the minimization of total loss, and P_{loss} was obtained using Equation (24). Parameters of the FA used for the simulation are Table 1.

Table 1: FA Simulation parameters

Values
33
1.0
1.0
0.01
100

D. Impact of DG Penetration on the Level Short Circuit Current

Penetration of multiple DGs increases the level of short circuit current in a distribution network. The level of short circuit current depends on the type of renewable energy source with the smallest fault been generated by generator excited by the stator. Convection overcurrent distribution relay network protection scheme is calibrated using the estimated short circuit current level and its effect studied with and without DG. Short circuit current was introduced in the different buses in the distribution network of IEEE 33bus and Ayepe 34-bus radial networks with and without DG and different level of short circuit current were calculated.

E. Simulation Power System Network

In this research, the standard IEEE 33-bus and Ayepe 34-bus distribution networks were used to test the developed hybrid technique using NEPLAN and DigSilent power factory software as simulation platforms as presented in Figures 2 and 3, respectively. The data for the IEEE 33-bus network was obtained from [19], and the data for the Avepe 34-bus network were sourced from the Ibadan Electricity Distribution Company of Nigeria (IBEDC) and are presented in Appendices A and B. The conventional and non-conventional sizing and placement of DG were modelled using MATLAB software. The network hybrid optimal location and sizing were equally modelled using MATLAB software.

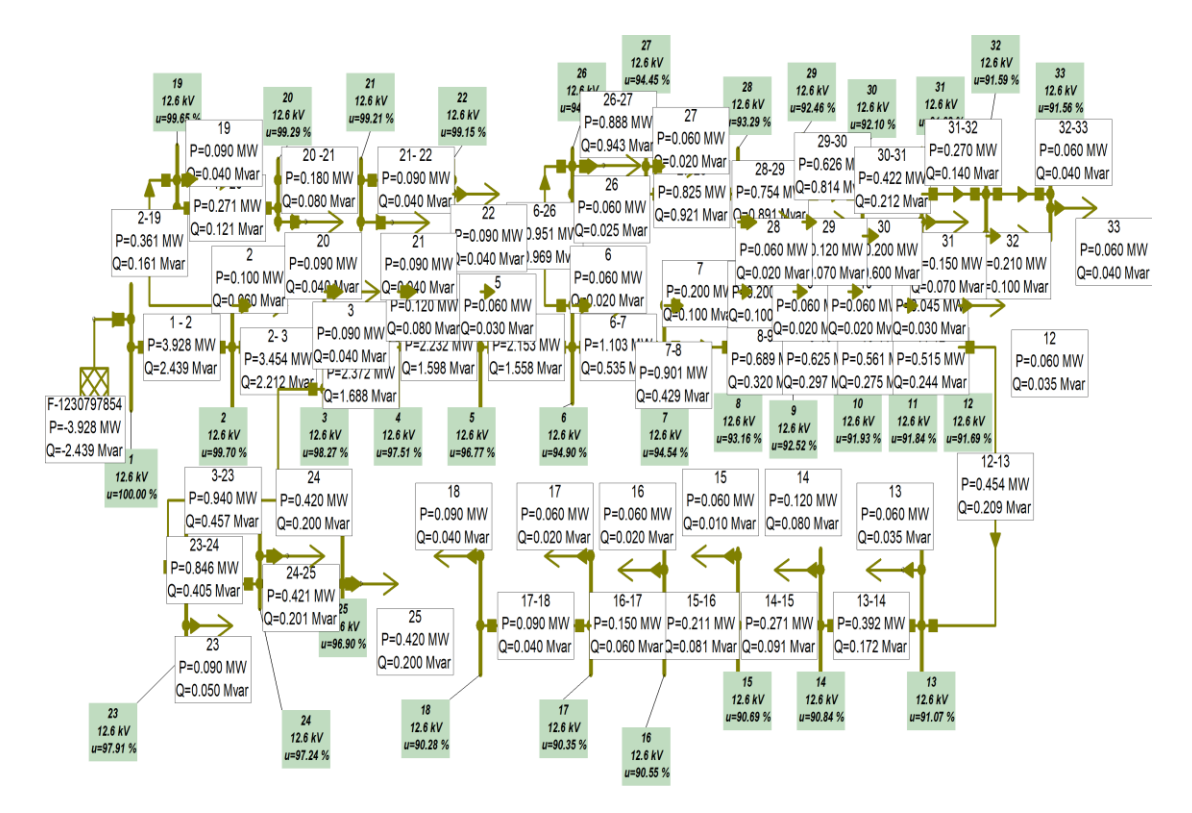


Figure 2: IEEE 33 Bus Distribution Network

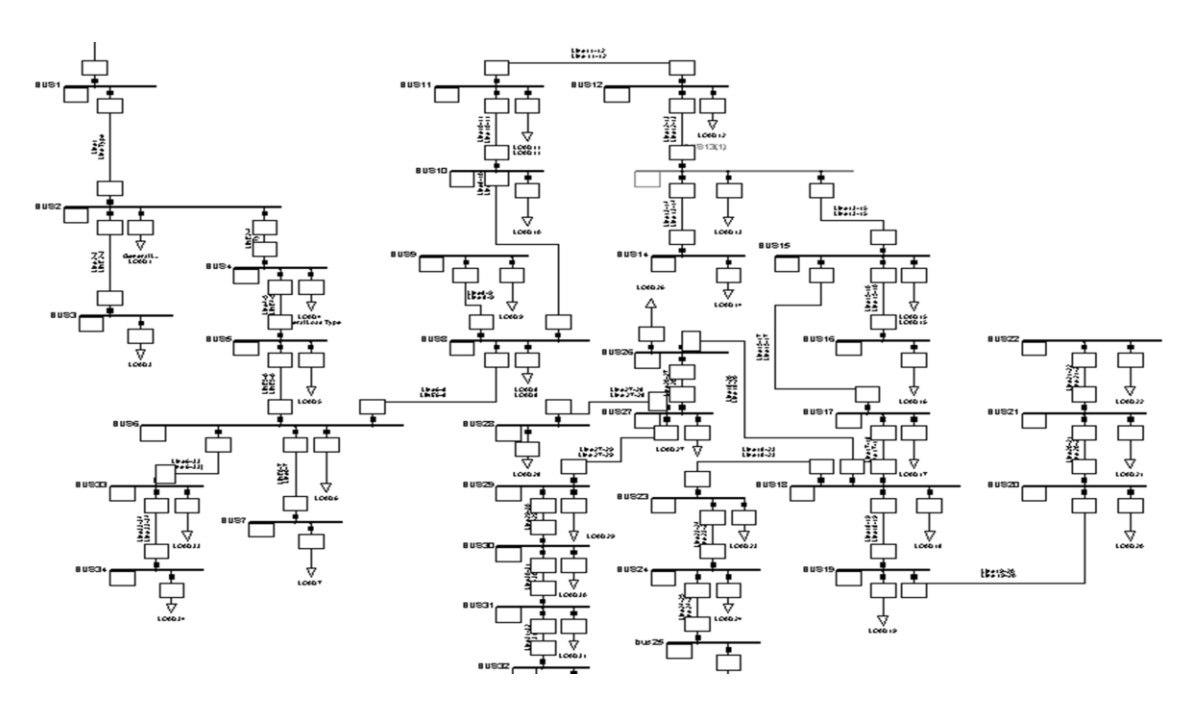


Figure 3: Ayepe 34 Bus Distribution Network

III. Results and Discussion

The base-case load flow solution was run on IEEE 33-bus and Ayepe 34-bus distribution systems as shown in Figures 4 and 5, respectively. The total real and reactive load demand for the IEEE 33-bus network were 3.715 MW and 2.295 MVar. The system real and reactive generating capacities were 3.928 MW and 2.439 MVar. The base case total real and reactive power losses obtained from the NEPLAN software were found to be 0.213 MW and 0.144 Mvar, respectively. The nodal voltage in percent with respect to the nominal node voltage as plotted in Figure 4 shows that the minimum bus voltage occurred at bus

number 18, which was 90.28%.

Similarly, for the Ayepe 34-bus network, the base case load flow analysis was carried out and the result indicated that voltage magnitude of some of the buses were below statutory voltage limits of ±5% of the nominal voltage magnitude. From the load flow analysis as presented in Figure 5, the voltage magnitudes below the acceptable lower voltage limit were observed from buses 9-32 with the minimum voltage magnitude of 0.924 occurring at bus 32. The total active and reactive power losses of the base case load flow analysis were 0.18 MW and 0.30 Mvar, respectively.

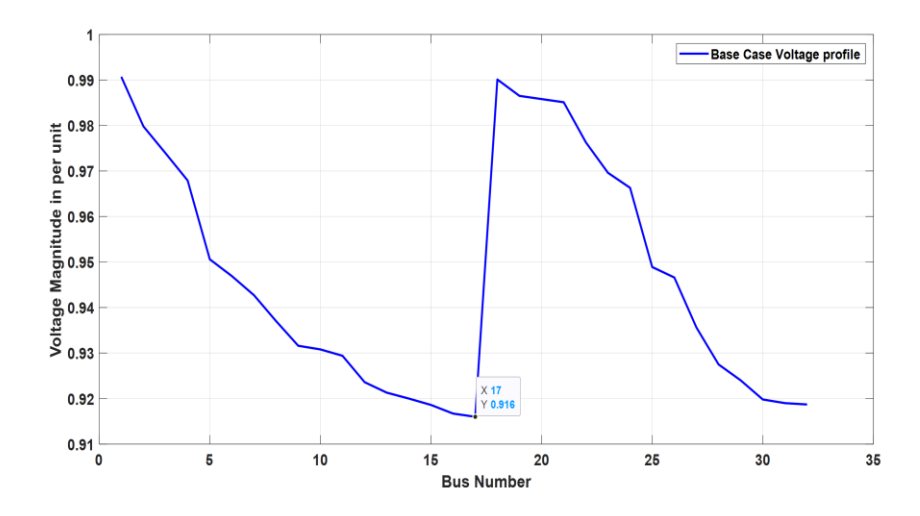


Figure 4: Base Case Voltage Profile for IEEE 33 Bus System Network

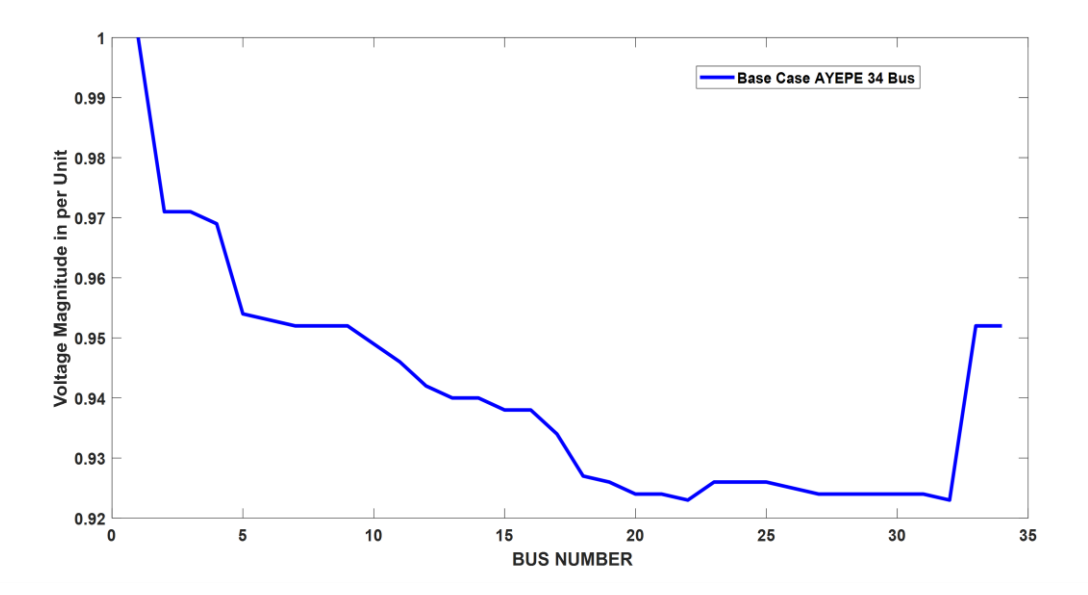


Figure 5. Base Case Voltage Profile for Ayepe 34-Bus Network

A. Conventional DG Placement and Sizing for the IEEE 33 and Ayepe 34-Bus

The conventional methods (PLSI and VSI) as presented in sections 2.1 and 2.2 were used for the DG placement and sizing, respectively. Figures 6 and 7 present a voltage profile resulting from the proper placement of DG in the IEEE 33-bus and Ayepe 34-bus distribution networks. Different sizes of DGs calculated using the Equation (22). DG units were introduced into the test networks at different buses. Based on the calculations, DG sizes of 3016.533 kW and 2564.070 kW were required for the IEEE 33-bus distribution network, with each being placed at buses 6 and 30, which were determined to be the optimal locations for the DG units, respectively. The bus with the lowest voltage magnitude, which was bus 18, had its voltage improved from 0.9036 to 0.9546 p.u., resulting in a 5.6% enhancement in the overall voltage profile. The total power loss was relatively reduced from

503 to 178 kW with DG placement at bus 6 and bus 30. This indicates a 64.61% reduction in the total real power loss as compared with the base case scenarios

For Avepe 34-bus network, the MATLAB simulation of DG sizing shows that the optimal sizes for DG units to be placed at buses 20 and 21 are 2005.1 kW and 1205 kW, respectively, which were determined as the optimal DG locations. The results of load flow analysis, which shows the plot of the voltage magnitudes are illustrated in Figure 7. The minimum voltage improved from 0.924 to 0.936 which is an indication of the positive effect of the DG that was integrated to the system. The real and reactive power losses were reduced from 0.18 MW and 0.30 Mvar to 0.14 MW and 0.23 Mvar, which indicates 22.2 and 23.3% reduction in total real and reactive power losses when compared the base case.

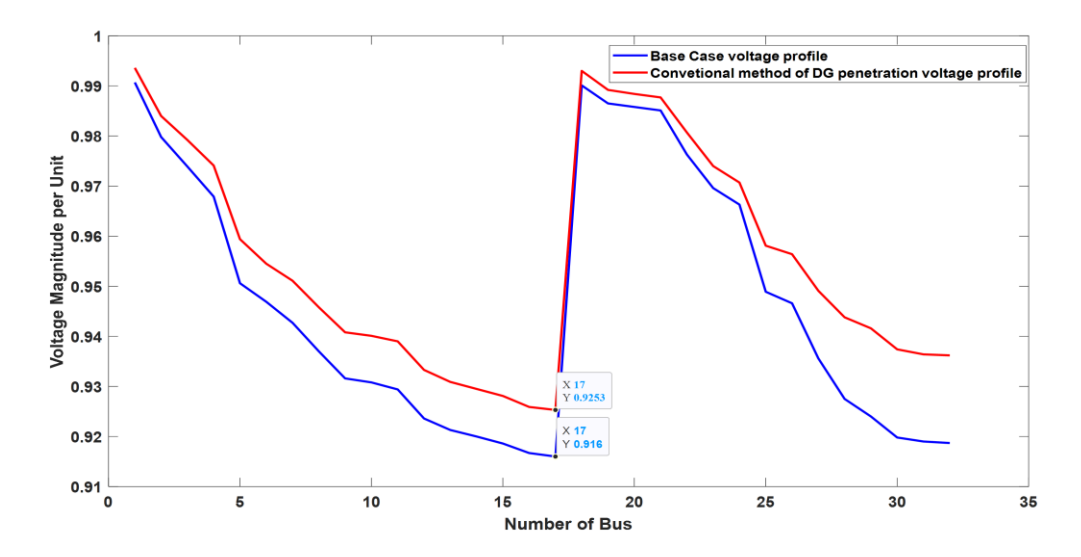


Figure 6. Voltage Profile of Base Case and Conventional DG Penetration for IEEE 33 Bus

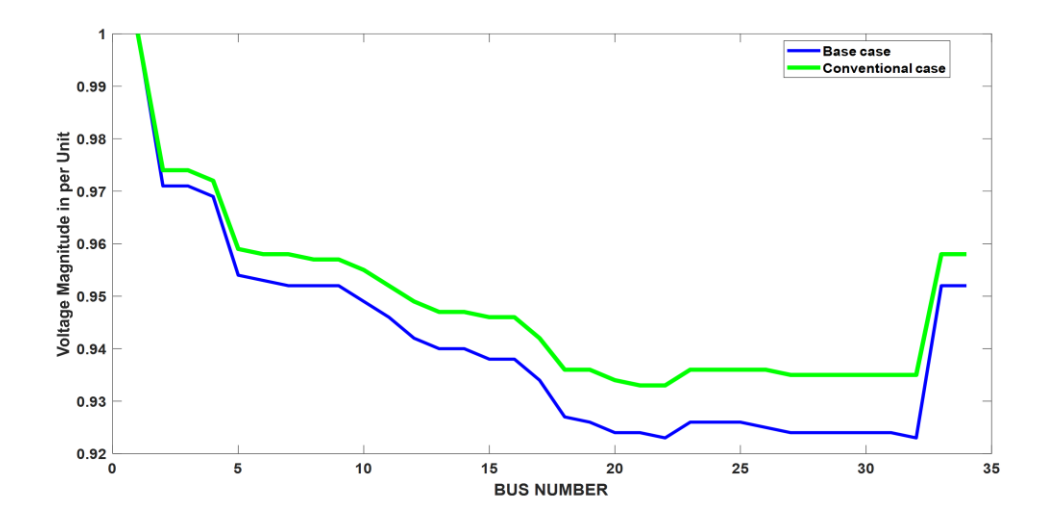


Figure 7: Voltage Profile of Base Case and Conventional DG Penetration for Ayepe 33

B. Hybrid Method of DG Placement Using Firefly Algorithm for IEEE 33 and Ayepe bus

The algorithm presented in section 2.3 was implemented for the hybrid model. The population size adopted were based on the total number of buses involved in the distribution networks (33-bus and Ayepe 34-bus). The optimal sizes of DG were calculated

using the conventional mathematical approach. The optimal DG location for the IEEE 33-bus distribution network were obtained to be at buses 3 and 28, respectively. The optimal sizes of DGs at these locations were 0.156 and 0.487 MW, respectively. The total real power loss after the DG units were placement at buses 3 and 28 was 0.134 MW and when compared the result with the base case power loss 0.213 MW

represent 37.09% reduction in the real power loss. From Figure 8, the voltage magnitude of the distribution network improved from 0.9164 to 0.9253 p.u. for the conventional method and 0.9346 p.u. for the hybrid algorithm.

For the Ayepe 34-bus distribution network, a hybrid simulation was performed and the result showed that bus 28 with 405 kW DG penetration produced a real and reactive power

loss of 0.06 MW and 0.10 Mvar. This shows a reduction in power lose from 0.18 MW and 0.30 Mvar for the base case to 0.14 MW and 0.23 Mvar for the conventional method. This represents 66.67% reduction in real power lose when compared with the base case and 57.14% when compared with the conventional method. Figure 9 shows an improvement in the voltage profile when the DG was integrated into the specified bus.

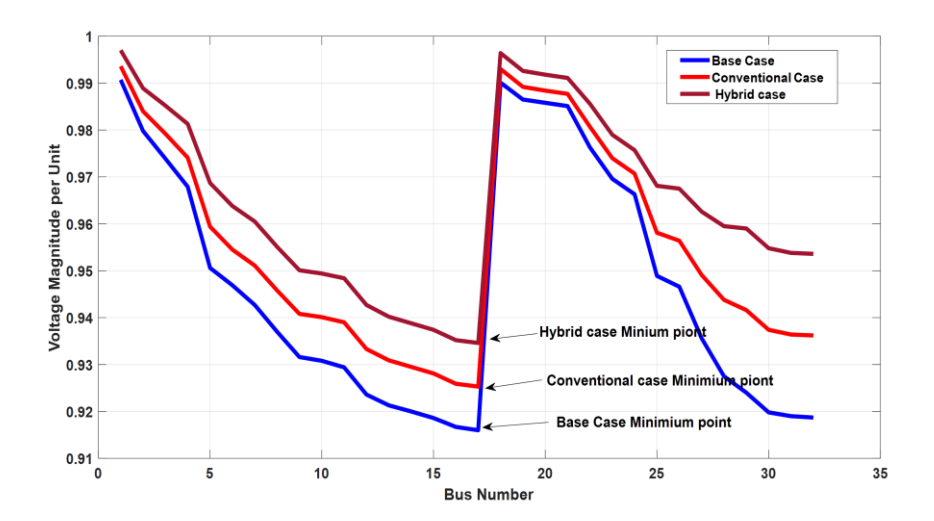


Figure 8. Voltage Magnitude of the IEEE 33 bus using Hybrid Model

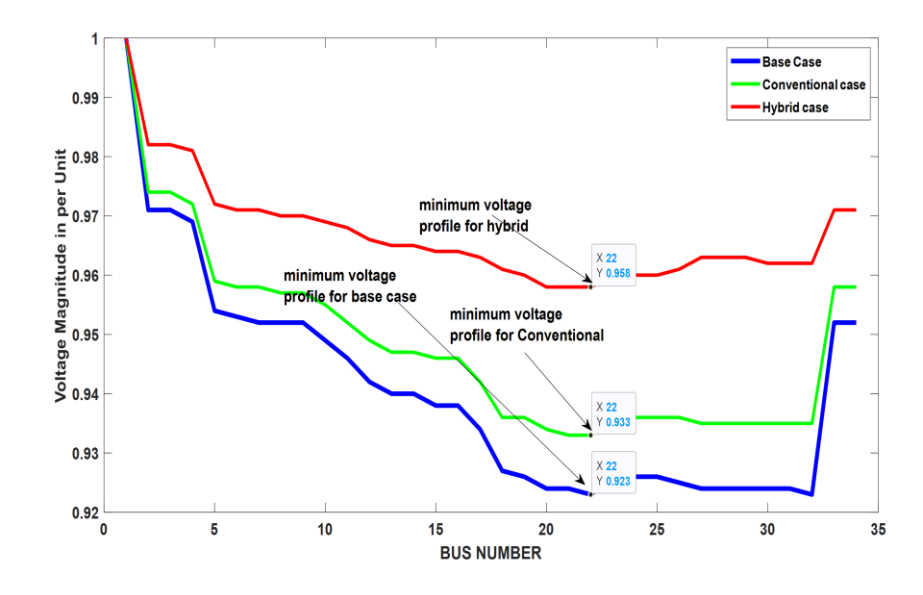


Figure 9: Voltage Magnitude of the Ayepe 33-Bus using Hybrid Model

C. Impact of DG Penetration on Short Circuit Current Level

The short circuit fault current analysis of the distribution network was performed both before and after DG penetration, and the results as presented in Figures 10 and 11. Thus, short-circuit fault current analysis constraint-based criterion that forms an exclusion principle for the selection of candidate buses for optimal location of DG in a distribution network. It can be observed that the strength of a bus is directly related to the short circuit level, the higher the short circuit level of the bus, the more it is able to maintain its voltage in case of a fault on any other bus.

The placement of DG in the distribution network is optimally located with elimination of buses with high level of short circuit current. Figure 10 shows the short-circuit current levels of the IEEE 33-bus system for the base case short-circuit current analysis. Buses 3 to 16, 18 to 20, and 22 to 31 exhibit low levels of short-circuit current, indicating an expected penetration of DG. After placing DG in bus 3 and 28 and performing another short circuit analysis as shown in Figure 11, the level of short circuit current increased from the maximum 21 kA at bus 17 to 38 kA at bus 19.

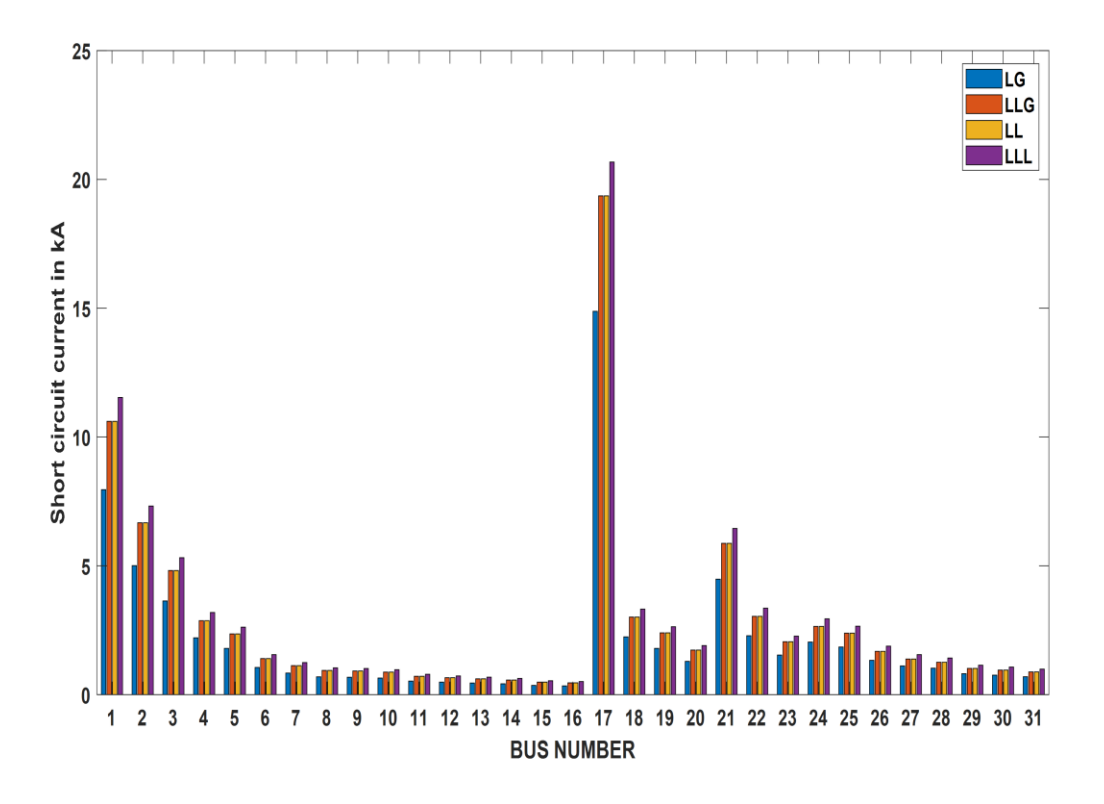
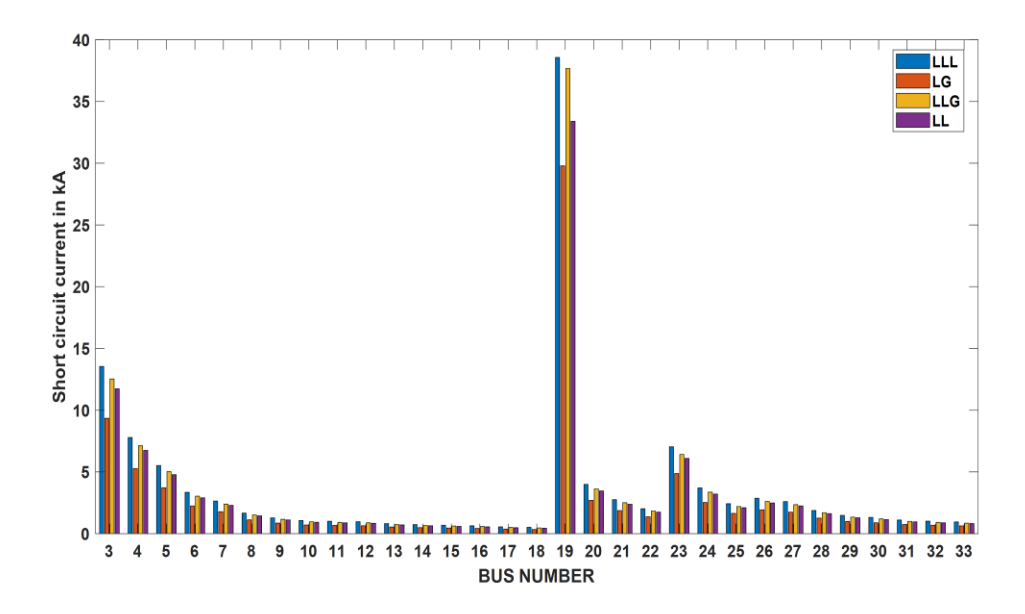


Figure 10: Base Case Short Circuit Current Level of IEEE 33 Bus



The short circuit fault current analysis of the Ayepe 34 bus distribution network performed both without and with penetration and the results as presented in Figures 12 to 13. the higher the short circuit level of the bus, the more it is able to maintain its voltage in case of a fault on any other bus. From Figure 12, buses 1, 3, 32, and 33 are more stable than other buses because of higher short circuit current hence, the need to increase the short circuit current of other buses by introducing DGs. Buses 4 to 31 require DG penetration which will improve the voltage profile of these buses and equally increase the level of short circuit current in these buses and equally increase its stability level. The procedure was adopted for the placement of DG which saw bus 28 the bus with the optimal performance. Figure 13 presents the different level of short circuit current after the placement of DG.

D. Impact of Increase of Short Circuit Current on Overcurrent Protection Systems

Two different simulations were carried out on the overcurrent protection relay connected to bus 4 without and with DG penetration on the IEEE 33-bus distribution network. Short circuit current was introduced in different location of the feeder 1 in the distribution network. Figure 14 presents the tripping information of the overcurrent relay without DG penetration. The results show that the preset relay, which is calibrated during installation by assuming the worst-case scenario trip at 0.22 seconds at 3 kA short circuit current. Figure 15 presents the tripping information of the overcurrent relay with the DG penetration. From Figure 15 it was observed that the overcurrent relay connected to bus 4 tripped at 0.35 seconds at 5 kA which definitely affected the entire overcurrent distribution network relay coordination. This increase altered the preset values and cause maloperation of a lot of relays connected to the distribution network.

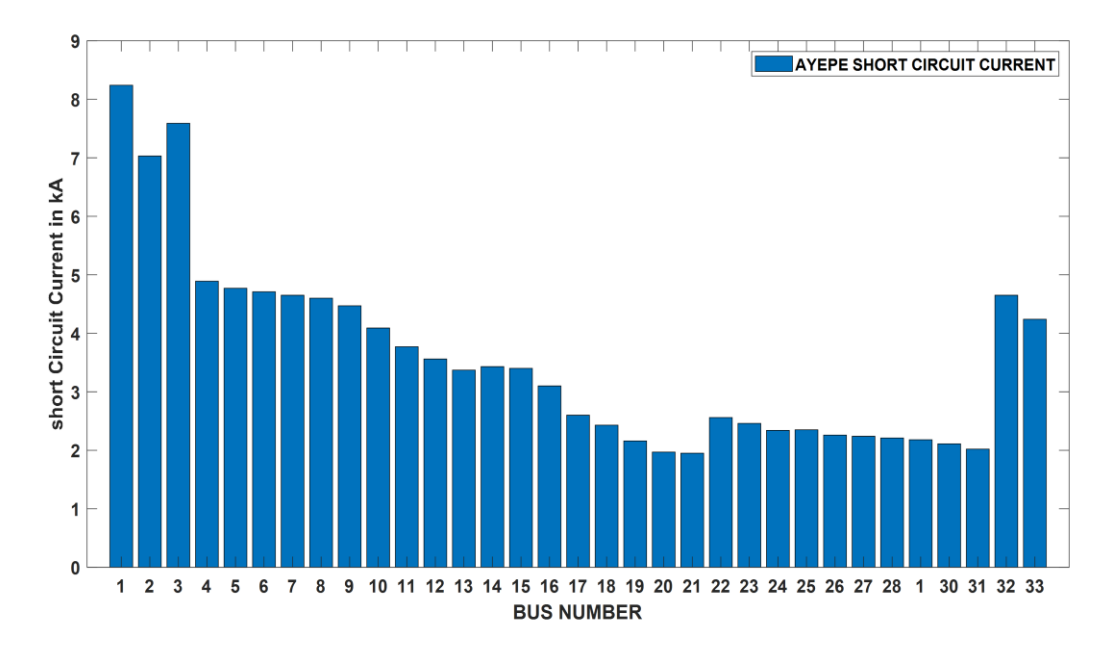


Figure 12: Base Case Short Circuit Current Level of Ayepe 34 Bus Network

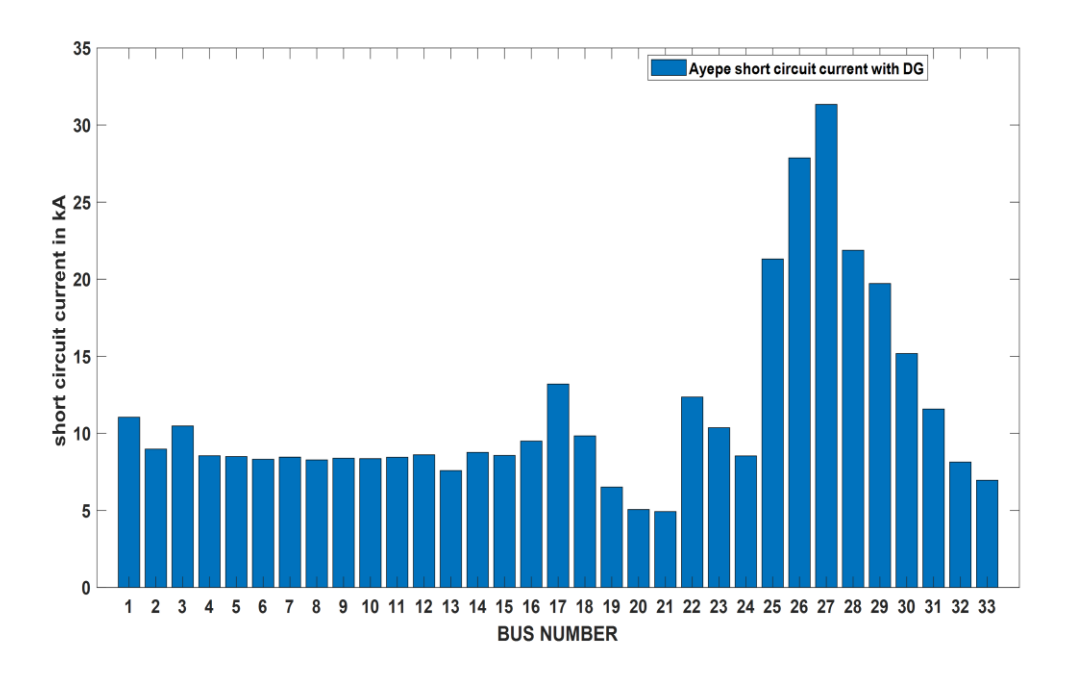


Figure 13: Short Circuit Current Level of Ayepe 34 Bus Network with DG

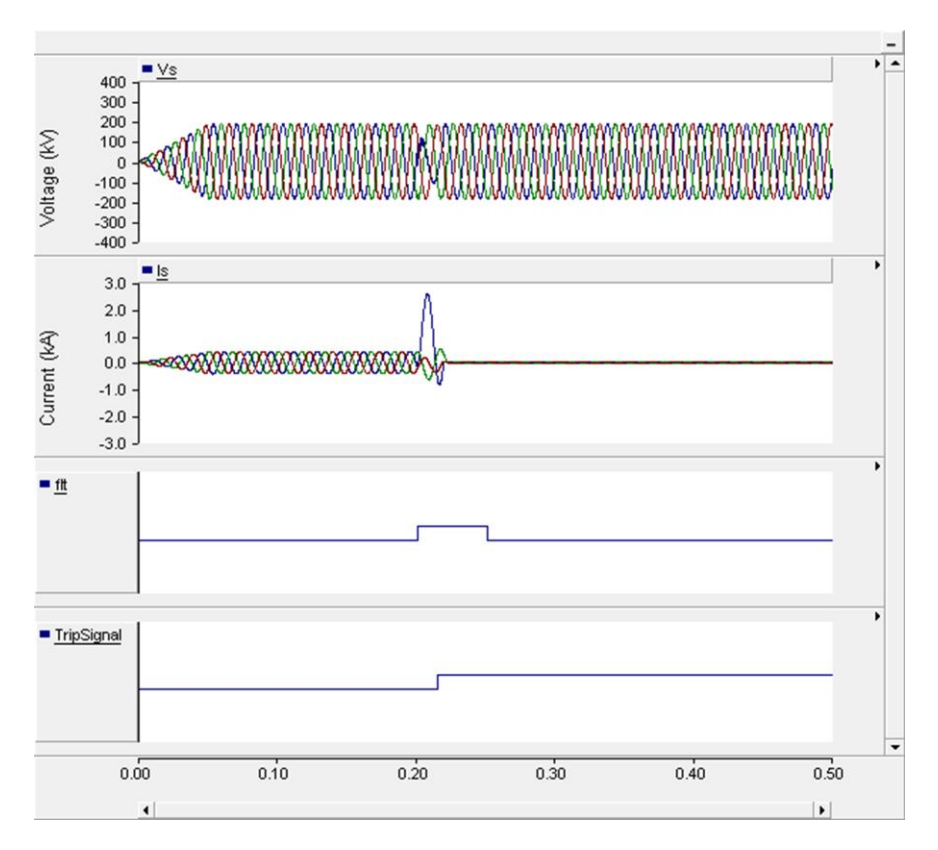


Figure 14: IEEE 33 Bus 4 Overcurrent Relay Trip Data without DG

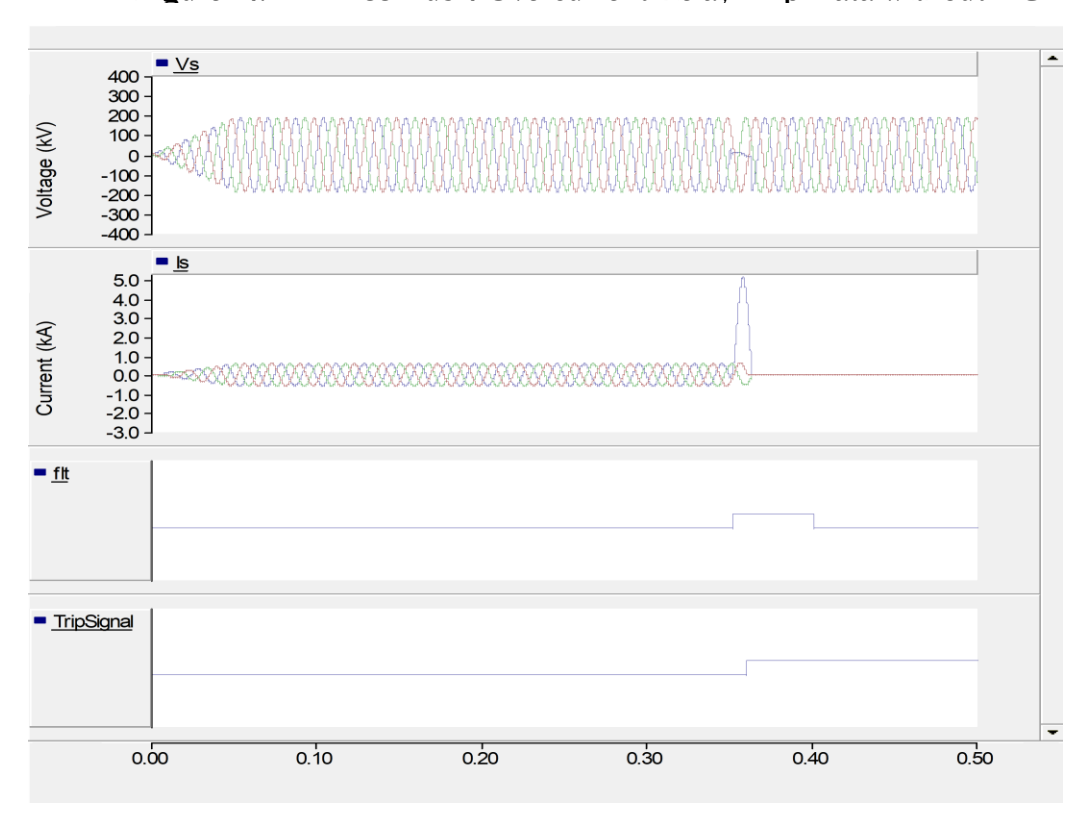


Figure 15. IEEE 33 Bus 4 Overcurrent Relay Trip Data with DG

IV. Conclusion

This paper has described the optimal location and sizing of DG in a typical distribution network using the FA and its impact on the network overcurrent relay coordination. The proposed hybrid method found the ideal DG locations and capacities to be buses 2 and 8, with 0.156 and 0.487 MW, respectively, causing a 37.09% reduction in loss. The conventional method applied to the Ayepe 34-bus radial distribution network generated 2005.1 and 1205 kW DGs at buses 20 and 21, respectively. The integration of these DGs reduced the total real and reactive power losses by 22.3% and 23.3%, respectively, while the hybrid reduced the real power loss by 66.67%. From the relay simulation, it showed that the conventional overcurrent protection scheme is affected by the penetration of DG units. The results obtained from the hybrid algorithm show a significant improvement from the existing results.

References

- [1] Che, L., M. E. Khodayar, and M. Shahidehpour, "Adaptive protection system for microgrids: Protection practices of a functional microgrid system," *IEEE Electrification Magazine*, vol. 2, no. 1, 2014, pp. 66–80.
- [2] Lakshmi, G. N., A. Jayalaxmi, and V. Veeramsetty, "Optimal placement of distributed generation using firefly algorithm," in *IOP Conference Series: Materials Science and Engineering*, vol. 981, no. 4, 2020, p. 042060.
- [3] Soudi, S., "Distribution system planning with distributed generations considering benefits and costs," *International Journal of Modern Education and Computer Science*, vol. 5, no. 9, 2013.

- Georgilakis, S., [4] Р. and N. D. "Optimal Hatziargyriou, distributed generation placement in power distribution networks: Models, methods, and future research," IEEE Transactions on Power Systems, vol. 28, no. 3, 2013, pp. 3420-3428.
- [5] Abou El-Ela, A. A., S. M. Allam, and M. M. Shatla, "Maximal optimal benefits of distributed generation using genetic algorithms," *Electric Power Systems* Research, vol. 80, no. 7, 2010, pp. 869–877.
- [6] Acharya, N., P. Mahat, and N. Mithulananthan, "An analytical approach for DG allocation in primary distribution network," *International Journal of Electrical Power and Energy Systems*, vol. 28, no. 10, 2006, pp. 669–678.
- [7] Hung, D. Q., and N. Mithulananthan, "Multiple distributed generator placement in primary distribution networks for loss reduction," *IEEE Transactions on Industrial Electronics*, vol. 60, no. 4, 2011, pp. 1700–1708.
- [8] Kim, J. O., S. W. Nam, S. K. Park, and C. Singh, "Dispersed generation planning using improved Hereford ranch algorithm," *Electric Power Systems Research*, vol. 47, no. 1, 1998, pp. 47–55.
- [9] Singh, D., D. Singh, and K. S. Verma, "GA based optimal sizing and placement of distributed generation for loss minimization," *International Journal of Electrical and Computer Engineering*, vol. 2, no. 8, 2007, pp. 556–562.
- [10] Abbagana, M., G. A. Bakare, and I. Mustapha, "Optimal placement and sizing of a distributed generator in a power distribution system using

- differential evolution," in Proceedings of the 1st International Technology, Education and Environment Conference, 2011, pp. 536–549.
- [11] Kayal, P., and C. K. Chanda, "A simple and fast approach for allocation and size evaluation of distributed generation," *International Journal of Energy and Environmental Engineering*, vol. 4, 2013, pp. 1–9.
- [12] Moradi, M. H., and M. Abedini, "A combination of genetic algorithm and particle swarm optimization for optimal DG location and sizing in distribution systems," *International Journal of Electrical Power and Energy Systems*, vol. 34, no. 1, 2012, pp. 66–74.
- [13] Martinez, J. A., and J. Martin-Arnedo, "Impact of distributed generation on distribution protection and power quality," in 2009 IEEE Power and Energy Society General Meeting, 2009, pp. 1–6.
- [14] Conti, S., "Analysis of distribution network protection issues in presence of dispersed generation," *Electric Power Systems Research*, vol. 79, no. 1, 2009, pp. 49–56.
- [15] Kılıçkıran, H. C., H. Akdemir, İ. Şengör, B. Kekezoğlu, and N. G. Paterakis, "A non-standard characteristic based protection scheme for distribution networks," *Energies*, vol. 11, no. 5, 2018, p. 1241.
- [16] Ndahepele, L., and S. Chowdhury, "Impact of distributed generation on traditional protection in distribution and transmission systems: A review," in 2020 IEEE PESIAS PowerAfrica, 2020, pp. 1–5.
- [17] Udgave, A. D., and H. T. Jadhav, "A review on distribution network

- protection with penetration of distributed generation," in 2015 IEEE 9th International Conference on Intelligent Systems and Control (ISCO), 2015, pp. 1–4.
- [18] Dai, F. T., "Impacts of distributed generation on protection and autoreclosing of distribution networks," 2010.
- [19] Al-Anbarri, K. A. A., and D. W. S. Majeed, "Reliable load flow method for radial distribution systems," *Journal of Engineering Development*, vol. 16, no. 2, 2012.

Appendix A

Bus Data of Ayepe 34-Bus Radial Distribution Networks

Bus	Pd	Qd	Bs	Type	Vm	Va	Base kV	Vmax	Vmin
1	0	0	0	3	1	0	11.00	1.05	0.95
2	200	100	0	3	1	0	11.00	1.05	0.95
3	200	100	0	3	1	0	11.00	1.05	0.95
4	120	50	0	3	1	0	11.00	1.05	0.95
5	120	50	0	3	1	0	11.00	1.05	0.95
6	120	50	0	3	1	0	11.00	1.05	0.95
7	120	50	0	3	1	0	11.00	1.05	0.95
8	23	15	0	3	1	0	11.00	1.05	0.95
9	200	100	0	3	1	0	11.00	1.05	0.95
10	45	30	0	3	1	0	11.00	1.05	0.95
11	120	50	0	3	1	0	11.00	1.05	0.95
12	23	15	0	3	1	0	11.00	1.05	0.95
13	45	30	0	3	1	0	11.00	1.05	0.95
14	135	90	0	3	1	0	11.00	1.05	0.95
15	200	100	0	3	1	0	11.00	1.05	0.95
16	23	15	0	3	1	0	11.00	1.05	0.95
17	200	100	0	3	1	0	11.00	1.05	0.95
18	200	100	0	3	1	0	11.00	1.05	0.95
19	200	100	0	3	1	0	11.00	1.05	0.95
20	120	50	0	3	1	0	11.00	1.05	0.95
21	200	100	0	3	1	0	11.00	1.05	0.95
22	120	50	0	3	1	0	11.00	1.05	0.95
23	120	50	0	3	1	0	11.00	1.05	0.95
24	200	100	0	3	1	0	11.00	1.05	0.95
25	120	50	0	3	1	0	11.00	1.05	0.95
26	200	100	0	3	1	0	11.00	1.05	0.95
27	120	60	0	3	1	0	11.00	1.05	0.95
28	120	60	0	3	1	0	11.00	1.05	0.95
29	40	30	0	3	1	0	11.00	1.05	0.95
30	120	60	0	3	1	0	11.00	1.05	0.95
31	120	60	0	3	1	0	11.00	1.05	0.95
32	80	60	0	3	1	0	11.00	1.05	0.95
33	120	60	0	3	1	0	11.00	1.05	0.95
34	23	15	0	3	1	0	11.00	1.05	0.95

 $\label{eq:Appendix B}$ Line Data of Ayepe 34-Bus Radial Distribution Networks

From	To	r (ohms)	x(ohms)	Status	Ratio	Rate A
1	2	0.41975	0.72266	1	0	9990
2	3	0.073	0.12568	1	0	9990
2	4	0.0365	0.06284	1	0	9990
4	5	0.2555	0.43988	1	0	9990
5	6	0.01825	0.03142	1	0	9990
6	7	0.00913	0.0152	1	0	9990
6	8	0.01825	0.03142	1	0	9990
8	9	0.00913	0.0157	1	0	9990
8	10	0.09125	0.0157	1	0	9990
10	11	0.073	0.12568	1	0	9990
11	12	0.073	0.12568	1	0	9990
12	13	0.05475	0.09426	1	0	9990
13	14	0.05475	0.09426	1	0	9990
13	15	0.0365	0.06284	1	0	9990
15	16	0.00913	0.01571	1	0	9990
15	17	0.1095	0.18852	1	0	9990
17	18	0.219	0.37704	1	0	9990
18	19	0.0913	0.1571	1	0	9990
19	20	0.1825	0.3142	1	0	9990
20	21	0.1552	0.26707	1	0	9990
21	22	0.01825	0.03142	1	0	9990
18	23	0.01825	0.03142	1	0	9990
23	24	0.05475	0.09426	1	0	9990
18	26	0.01825	0.3142	1	0	9990
26	27	0.1825	0.03142	1	0	9990
27	28	0.01825	0.03142	1	0	9990
27	29	0.0365	0.06284	1	0	9990
29	30	0.01825	0.03142	1	0	9990
30	31	0.05475	0.09426	1	0	9990
31	32	0.073	0.12568	1	0	9990